Geometric reasoning about damped and forced harmonic motion in the complex plane

Hunter G. Close
Department of Physics, Texas State University, San Marcos, Texas 78666

(Received 30 March 2014; accepted 23 June 2015)

Complex-valued functions are commonly used to solve differential equations for one-dimensional motion of a harmonic oscillator with linear damping, a sinusoidal driving force, or both. However, the usual approach treats complex functions as an algebraic shortcut, neglecting geometrical representations of those functions and discarding imaginary parts. This article emphasizes the benefit of using diagrams in the complex plane for such systems, in order to build intuition about harmonic motion and promote spatial reasoning and the use of varied representations. Examples include the analysis of exact time sequences of various kinematic events in damped harmonic motion, sense-making about the phase difference between a driving force and the resulting motion, and understanding the discrepancy between the resonant frequency and the natural undamped frequency for forced, damped harmonic motion. The approach is suitable for supporting instruction in undergraduate upper-division classical mechanics.
[http://dx.doi.org/10.1119/1.4923439]

I. INTRODUCTION

Instruction on oscillations often employs complex-valued functions like $Ae^{i(\omega t-\phi)}$ to find position vs time solutions for simple, damped, and driven oscillatory systems. In upper-division courses on classical mechanics, very seldom do textbooks begin to explore geometrical interpretations of these complex functions by depicting solutions in the complex plane, or further use these constructions as a basis for analysis. In introductory calculus-based physics instruction on ac circuits, by contrast, it is common to show a "phasor" representation of oscillatory quantities (i.e., showing the quantities as arrows rotating in an abstract plane). Even these treatments, however, only scratch the surface of what can be discovered through an intellectual inhabitation of the complex plane. In this article, I show some of the insight into the mathematics of oscillation that can be gained through a geometrical perspective. In this way, the geometrical approach can be seen as complementary to algebraic reasoning and physical reasoning.

The work presented here is not a systematic empirical study of student learning, though it was developed through the experience of teaching classical mechanics over several years. At present, there have been no published empirical studies reporting specifically on student difficulties with the topic of damped and forced harmonic motion. The ideas of this article are presented for two purposes: (1) to enhance the physics education community's repertoire for teaching oscillations, and (2) to serve as a reference, by providing instructional context, for *future* formal empirical studies in physics education research. In particular, the addition of opportunities for students and instructors to engage with the mathematics of oscillations through time-dependent geometrical forms lays essential groundwork for embodied-action studies, which is a field of rich research opportunities in STEM learning.[1]

Physics education research studies on the use of multiple representations in instruction agree generally that using multiple representations in instruction has positive outcomes[2,3] for students, especially when their use is well-coordinated[4] and goal-directed.[5] Most such studies have been at the introductory level, though some instructional programs have aimed to extend the use of multiple representations (along with other basic reform characteristics like increased interactivity, metacognition, etc.) into the upper division, and have produced some research indicating that the reforms were called for and were positively effective.[6–10] It is therefore a premise of this article that the extension of typical treatments of topics to include rigorous reasoning using alternative representations is likely to contribute positively to the quality of instruction.

II. REVIEW OF TEXTBOOKS' USE OF THE COMPLEX PLANE FOR INSTRUCTION ON OSCILLATIONS

Since there is an existing tradition in physics education of treating oscillations with complex numbers and arrow depictions of phasors, I review some common treatments of the subject to show to what degree oscillations have been depicted in the complex plane, especially from the point of view of upper-division (or higher) classical mechanics.

In a review of 18 textbooks on classical mechanics, I found very few depictions of complex-valued kinematic variables or forces in the complex plane. For example, in one currently popular text,[11] complex exponential solutions for simple harmonic motion and for a generic second-order linear inhomogeneous equation are treated in an Appendix rather than in the chapter on harmonic motion. This Appendix also includes a diagram of a phase angle located in a triangle, but otherwise does not depict complex solutions. Another popular text[12] shows complex exponential solutions for simple harmonic motion, including a diagram of the phasor representing the complex position $\tilde{x}(t)$ at an arbitrary instant in time. It also shows complex exponential solutions for damped, unforced harmonic motion, and for damped, forced harmonic motion, but only in algebraic form, except for a triangle[13] that illustrates the relationship between the phase angle and various frequency-type quantities.

I also reviewed the use of the complex plane for describing and explaining oscillations in two commonly used introductory calculus-based physics texts.[14] In both, no explicit

mention is made of complex numbers per se; however, both texts also show "phasors" for the treatment of ac circuits, especially in the case of sinusoidally driven *RLC* circuits. The phasors are not explained in terms of complex numbers but rather through analogy to the relationship between uniform circular motion and simple harmonic motion. As might be expected, these introductory treatments do not address fine quantitative issues relating to timing, phase, and driving frequency.

III. SCOPE OF GEOMETRIC REASONING IN THE COMPLEX PLANE

The following approach to understanding oscillations emphasizes graphing complex functions of time in the complex plane using an arrow representation. These complex functions are determined through some algebraic work and then graphed in preparation for geometric reasoning.

All systems considered here consist of at least a mass connected to an ideal spring that is fixed to a wall. The spring constant is never varied. The damping is exclusively *linear* (i.e., drag force proportional to velocity, or $F_{\text{drag}} = -bv$). Further, this damping is restricted to *under-damped* rather than critically damped or over-damped conditions, but the damping is *non-negligible*. For "forced" systems, both undamped and underdamped systems are considered, and the driving force is sinusoidal. In the case of undamped, forced harmonic motion, the driving frequency is any frequency *except* the natural undamped frequency.

The following analysis is organized around three questions:

Question 1:
In underdamped harmonic motion, by what extra-algebraic means can we know when exactly an oscillator released from rest (a) has maximum speed and (b) passes through equilibrium, in relation to the lapsing of one-quarter period?
Question 2:
In forced, damped harmonic motion, what sense can we make of the relationship between the driving frequency and the phase angle $\phi(\omega)$ *between the driving force and the resulting motion*?
Question 3:
In forced, damped harmonic motion, why does resonance happen at a frequency that is less than the undamped, natural frequency of motion?

IV. UNDERDAMPED HARMONIC MOTION

When linear damping is introduced to a simple harmonic oscillator, we try a solution of the form $\tilde{x}(t) = Ae^{\zeta t - i\phi}$, anticipating that if the "frequency" ζ has nonzero real and imaginary parts, the solution will have corresponding exponential decay and sinusoidal factors, respectively. As with simple harmonic motion, time derivatives effectively multiply the original function by the complex exponent ζ, so that $\dot{\tilde{x}} = \zeta\tilde{x}$ and $\ddot{\tilde{x}} = \zeta\dot{\tilde{x}} = \zeta^2\tilde{x}$. Geometrically, this multiplication results in a change in amplitude and phase. To determine the extent of the phase-shift aspect of this multiplication, we substitute $\ddot{\tilde{x}} = \zeta\dot{\tilde{x}} = \zeta^2\tilde{x}$ into the equation of motion and find that

$$\zeta = \frac{-b}{2m} \pm i\sqrt{\frac{k}{m} - \left(\frac{b}{2m}\right)^2} = -\gamma \pm i\sqrt{\omega_0^2 - \gamma^2}$$
$$= -\gamma \pm i\omega_d, \tag{1}$$

with $\gamma = b/2m$ and $\omega_d = \sqrt{\omega_0^2 - \gamma^2}$. These two solutions for ζ differ by the sign of the imaginary component, which is not physically distinguishable, so we can proceed using $\zeta = -\gamma + i\omega_d$.

Taking the absolute magnitude gives $|\zeta| = |-\gamma + i\omega_d| = \sqrt{\gamma^2 + \omega_d^2} = \sqrt{\gamma^2 + (\omega_0^2 - \gamma^2)} = \omega_0$, which means that the complex frequency ζ has the same magnitude as the original undamped frequency ω_0. Noticing that the phase angle of ζ must be between $\pi/2$ and π (because of the positive imaginary component and the negative real component), we can rewrite ζ in polar form as $\zeta = \omega_0 e^{i(\pi/2+\delta)}$, giving

$$\ddot{\tilde{x}} = \zeta\dot{\tilde{x}} = \omega_0 e^{i\left(\frac{\pi}{2}+\delta\right)}\dot{\tilde{x}} = \zeta^2\tilde{x} = \omega_0^2 e^{i\left[2\left(\frac{\pi}{2}+\delta\right)\right]}\tilde{x}. \tag{2}$$

Geometrically, each time derivative results in a counterclockwise phase shift of $\pi/2 + \delta$, where

$$\delta = \tan^{-1}\left(\frac{\gamma}{\omega_d}\right) = \tan^{-1}\left(\frac{\gamma}{\sqrt{\omega_0^2 - \gamma^2}}\right), \tag{3}$$

as is apparent from Fig. 1(a). Note that in the absence of damping, δ approaches zero and the angle between adjacent arrows approaches $\pi/2$, yielding a diagram for the case of simple harmonic motion.

Figure 1(a) shows the ζ plane, where locations represent complex frequencies. The complex frequency ζ is shown in order to illustrate the phase angle that separates the complex kinematic variables in Fig. 1(b). The relative phase angles of position, velocity, and acceleration are constant, so the three of them can be understood as forming a rigid object. If this rigid object is modeled with pipe cleaners, for example, then the manipulative has the advantage of being posable, so the relative phase angle can be adjusted from one scenario to the next (if the damping constant is adjusted) while being held in a stable arrangement during the phase rotation of each scenario. Note also, however, that the complex kinematic variables also decay exponentially in magnitude over time, which would not be represented well with such a manipulative.

Figures 2(a)–2(f) show the phase angles of the kinematic variables at several key instants during damped harmonic motion. In Fig. 2(a), the phase angles are oriented to give zero real velocity, representing the oscillator starting from rest. This situation may already present a puzzle to students: How can the observable position $x(t)$ be maximum if the complex position $\tilde{x}(t)$ is not entirely real? If students can be led to consider this puzzle, a good opportunity arises for them to recognize the true definition of extremum in terms of zero derivative and to reconcile this understanding with the exponential decay of the magnitude of $\tilde{x}(t)$. By this path, students may come to realize that the real projection $x(t)$ can be, and is, maximized *before* $\tilde{x}(t)$ aligns with the real axis, which is shown in Fig. 2(b). Students can also be invited to wonder how the instant in Fig. 2(b) corresponds to a graph of $x(t)$ in relation to the envelope of exponential decay (they are mutually tangent), or to the observable motion in a lab (there is no corresponding special event). In Fig. 2(c), the

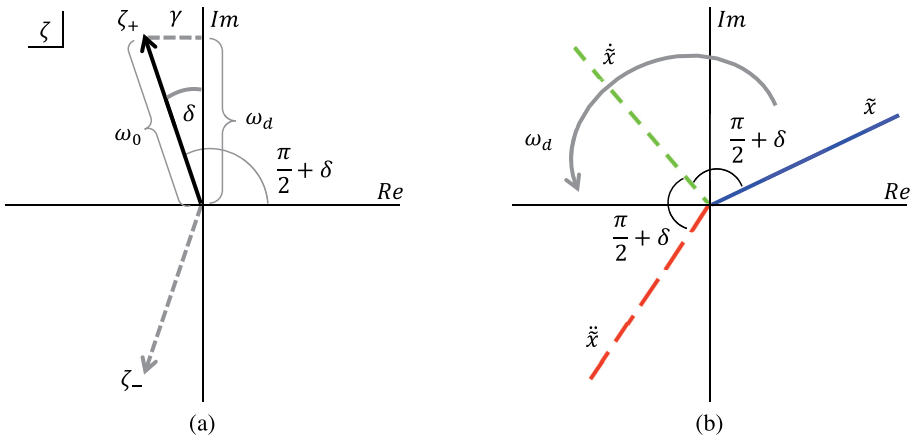

Fig. 1. (a) The zeta plane, where complex frequencies lie. The phase angle of ζ is $\pi/2+\delta$. Both roots ζ_+ and ζ_- are shown, but ζ_- is discarded. (b) The resulting phase angles for position, velocity, and acceleration at some arbitrary instant during the motion, which involves rotation at constant angular frequency ω_d and exponential decay of the magnitudes in time. Only the phase angles are shown; the magnitude information is omitted.

real part of the acceleration is zero, corresponding to an instant of maximum speed. Figure 2(d) represents the passage of one quarter period after release from rest. In Fig. 2(e), the real part of position is zero, so the oscillator has reached the equilibrium position. By comparing panels (c)–(e) in Fig. 2 we have an answer to Question 1: The instant of maximum speed occurs before one quarter period, and the instant of passing the equilibrium position occurs after one quarter period, *by the same interval of time*. This is seen by noting that the phase angle difference between panels (c) and (d) is the same as between panels (d) and (e) and remembering that the phase angles advance at a constant rate. Figure 2(f) shows the beginning of the next half-cycle, in which the pattern from (a)–(e) repeats.

Figure 3 shows graphs of the real components of position and velocity as functions of time. The instants of maximum speed and passing through the equilibrium position are marked to show the results from the geometric argument presented above.

There are good reasons to suppose that it is helpful for mathematical understanding to represent time-dependent kinematic variables and forces in oscillation as projections of objects that themselves form a rigid structure. Sfard[15] explains that there is a natural interplay in mathematical thinking and problem-solving between "operational and structural versions of the same mathematical ideas" (p. 28). The structural, or more object-like, version is more useful during a kind of cognitive "look-up" process, in which many characteristics of the idea are apprehended quickly and used to judge whether the operational or procedural aspects are worth recalling and expanding into the conscious awareness. From the vantage of experimental psychology, Schwartz and

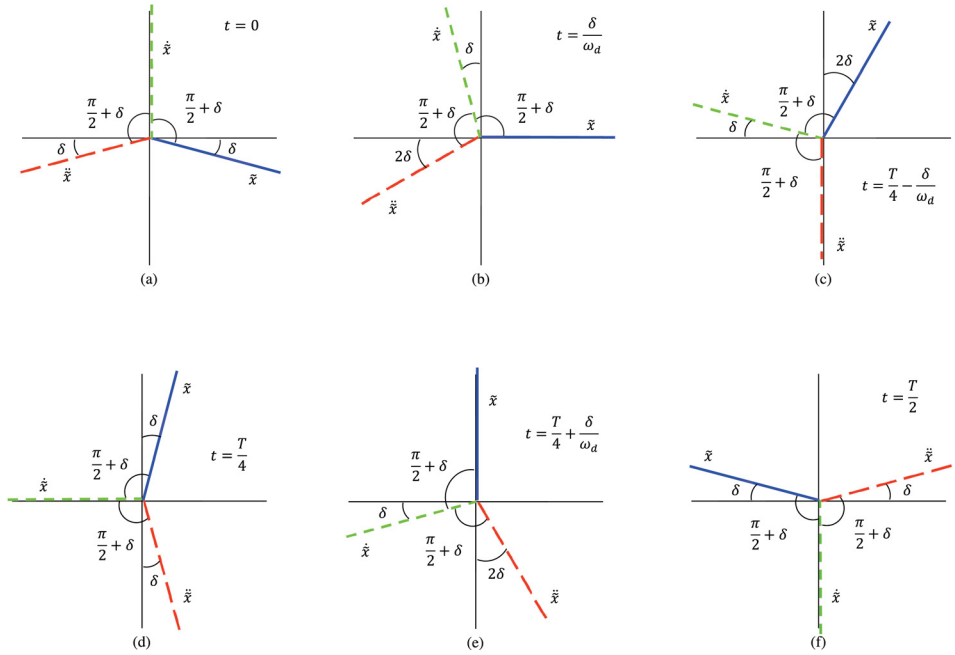

Fig. 2. Phase angles for complex position (blue dots), velocity (green small dashes), and acceleration (red large dashes) for six different instants during damped harmonic motion, in chronological order. (a) The oscillator is released from rest at a non-equilibrium position; (b) the complex position is purely real; (c) the acceleration is purely imaginary, so the oscillator has achieved maximum speed; (d) one quarter period has elapsed since release; (e) the oscillator passes through the equilibrium position; (f) one half period has elapsed, at which time the sequence in parts (a)–(e) repeats.

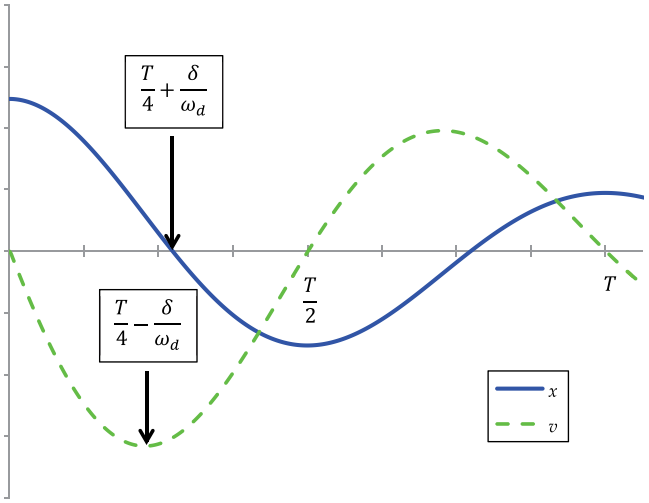

Fig. 3. Graphs of position and velocity as functions of time for underdamped oscillatory motion. The time at which the oscillator passes through the equilibrium position is *after* one quarter period, by an amount that is exactly equal to the amount of time that the instant of maximum speed comes *before* one quarter period.

Black showed[16] the natural back-and-forth between thinking in terms of rules of procedure and in terms of depictive models that people do when either becomes more efficient than the other for problem-solving. Thus, we can expect the complex-plane structures shown in Fig. 1 and later figures to serve the same kinds of functions for students when thinking about oscillations, in relation to other rule-based or procedural knowledge, like computing new algebraic expressions.

Visualization of the posable phase angle structure of the complex kinematic variables as shown in Fig. 2 can provide a geometric schema with which one can make various inferences relatively quickly, especially when used in conjunction with certain basic algebraic results. For instance, if the damping constant were increased, how would the graphs in Fig. 3 change? The angles separating position, velocity, and acceleration in Fig. 2 would spread while remaining equal to each other, and the rate of rotation of the structure would decrease. Thus, the graphs in Fig. 3 would be extended in time, and the time differences between the instants of zero position, quarter period, and maximum speed would increase in *greater* proportion than the increase in period, because the time disparity would cover a greater *fraction* of the cycle. Of course, understanding *why* the phase angle structure is what it is does require some basis of algebraic reasoning, as least as it has been presented here. Thus, the example here illustrates the benefit not of replacing one kind of reasoning with another but of strategic coordination of multiple lines of reasoning.

V. POSITION AMPLITUDE *A* AS PARAMETER AND DRIVING FORCE AMPLITUDE *F* AS FUNCTION

Typically, the sinusoidal driving force $F_{\text{driver}}(t) = F_0 \cos \omega t$ is modeled as having an amplitude of driving force that is an independently controlled parameter F_0. An alternative perspective of the relationship between driving force and position in forced oscillations, whether undamped or damped, is to imagine that the force amplitude F_0 is a dependent variable, not a fixed parameter (so, henceforth denoted just F, for brevity), while the position amplitude A is fixed, not variable (so, henceforth denoted A_0). In an electrical system, it is easy to imagine holding a fixed amplitude V_0 for a driving time-dependent voltage $\tilde{V}(t) = V_0 e^{i\omega t}$ and measuring the frequency-dependent response of, say, the voltage across a capacitor; however, for a mechanical system, in which we imagine the time-varying force as exerted by contact, the force amplitude of that oscillation might be harder to control directly. One can imagine instead that the oscillation is visually monitored so that the force amplitude is adjusted to achieve a set position amplitude A_0.

When the displacement amplitude is conceived as a function of frequency ω and the force parameter F_0, steady-state oscillations have an amplitude given by

$$A(\omega) = \frac{F_0/m}{\sqrt{(2\gamma\omega)^2 + \left(\omega_0^2 - \omega^2\right)^2}}. \tag{4}$$

In the case of fixed displacement amplitude A_0 and variable force amplitude $F(\omega)$, the resonant condition is defined as that driving frequency that requires the least force amplitude F. It is apparent from Eq. (4) that F has a functional dependence on ω that is the multiplicative inverse of that for the variable amplitude $A(\omega)$, namely

$$F(\omega) = mA_0\sqrt{(2\gamma\omega)^2 + (\omega_0^2 - \omega^2)^2}. \tag{5}$$

While $A(\omega)$ (with fixed F_0) is some finite value at $\omega = 0$, grows to a large finite value at $\omega = \omega_r$, and approaches zero as $\omega \to \infty$, $F(\omega)$ is some finite value at $\omega = 0$, shrinks to a relatively small finite value at $\omega = \omega_r$, and approaches infinity as $\omega \to \infty$ (see the top part of Fig. 8). This perspective, with fixed position amplitude A_0 and therefore fixed spring force amplitude $|\tilde{F}_{\text{spring}}| = m\omega_0^2 A_0$, is used in Secs. VI and VII to explore the geometric relationships among complex force phasors for variable frequency ω.

VI. UNDAMPED FORCED HARMONIC MOTION

If the damping is removed from the oscillator, and a sinusoidal driving force is applied, there is a steady-state sinusoidal motion of the system at the driving frequency with a phase difference between the force and the position of either 0 or π (see Fig. 4). The depiction of phasors in the complex plane to represent the forces helps to explain why the solution makes sense in terms of the same sort of vector-based reasoning that students are expected to do in introductory mechanics.

Newton's second law gives $\tilde{F}_{\text{spring}} + \tilde{F}_{\text{driver}}(t) = \Sigma\tilde{F} = m\ddot{\tilde{x}}$, which in this example has the form $-k\tilde{x} + Fe^{i\omega t} = m\ddot{\tilde{x}}$. Trying a steady-state phasor solution $\tilde{x}(t) = A_0 e^{i(\omega t - \phi)}$ yields the relation $F = m(\omega_0^2 - \omega^2)A_0 e^{-i\phi}$. Every part of the equation is real except possibly for $e^{-i\phi}$, which means $e^{-i\phi}$ is real. Thus, $\phi = 0$ or π. In this formulation, A_0 is strictly positive and the sign variation occurs only in the factors $e^{-i\phi}$ and $\omega_0^2 - \omega^2$. Figure 5 shows the two possibilities for the basic arrangement of force phasors in the cases $\phi = 0$ [Fig. 5(a)] and $\phi = \pi$ [Fig. 5(b)], which correspond to low ($\omega < \omega_0$) and high ($\omega > \omega_0$) driving frequencies, respectively. The phasors are shown at some instant for which the position has a purely positive real value, and the whole phasor diagram can be imagined to rotate counterclockwise as a rigid structure around the origin at frequency ω. The relatively simple network of geometric

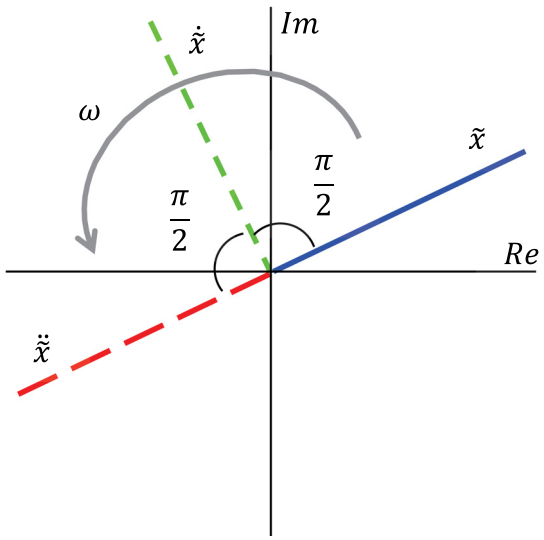

Fig. 4. Phase angles for position, velocity, and acceleration at an arbitrary instant for the steady-state solution to the harmonic oscillator with no damping and with a sinusoidal driving force.

interrelationships allows for a variety of paths of reasoning. For example, if the position is sinusoidal, then the acceleration phasor is directed exactly opposite the position phasor. The spring force phasor is also directed opposite to the position by $\tilde{F}_{\text{spring}} = -k\tilde{x}$. The net force phasor must be parallel to the acceleration phasor, and therefore to the spring force phasor. However, the spring force and net force phasors will generally not be the same length; the driving force phasor makes up the vector difference either way, depending on whether the driving frequency ω is lower or higher than the natural frequency ω_0. In either case, it is easy to see in this representation that the driving force must lie on the same line as the spring force in order to give a net force that is in the same direction as the spring force. This is another way of making sense of the result that the phase angle must be 0 or π. Similarly, one can reason that the effect of the driver in this scenario is simply to augment or reduce the spring constant.

VII. DAMPED FORCED HARMONIC MOTION

The "free-body diagram style" reasoning from Sec. VI is extended here by adding a linear damping force. In Fig. 6, four phasors are shown: one for each of three complex forces, due to the spring, the drag, and the driver; and the net force, which is the vector sum of the other three. The forces are shown at an arbitrary instant during steady-state motion in which the complex forces all have constant magnitude and constant relative phase angle; i.e., they form a rigid structure. The driving force is also shown as the sum of two components: one sharing an axis with the drag force, and one sharing an axis with the spring and net forces. In the example shown in Fig. 6, the net force is larger in magnitude than the spring force, which corresponds to the frequency of motion ω being greater than the natural frequency ω_0.

A. Making sense of $\phi(\omega)$ with the $\tilde{F}$ complex plane

The phasor diagram in Fig. 6 can be studied by varying the driving frequency ω and examining both the resulting phase angle $\phi(\omega)$ by which the driving force leads the position and the magnitude of the driving force in relation to the other forces. In Fig. 7, the complex forces from Fig. 6 are shown for particular values of ω: (a) very low frequency, (b) resonant frequency ω_r, (c) natural frequency ω_0, and (d) very high frequency. As in Fig. 5, the phasors in Fig. 7 are shown at some instant for which the position is a purely positive, real value.

For very low frequency, the drag force and net force magnitude can each be compared with the magnitude of the spring force:

$$|\tilde{F}_{\text{drag}}| = b\omega A_0 = b\omega \frac{|\tilde{F}_{\text{spring}}|}{m\omega_0^2} \propto \left(\frac{\omega}{\omega_0}\right)|\tilde{F}_{\text{spring}}| \approx 0, \tag{6}$$

$$|\Sigma\tilde{F}| = m\omega^2 A_0 = m\omega^2 \frac{|\tilde{F}_{\text{spring}}|}{m\omega_0^2} \propto \left(\frac{\omega}{\omega_0}\right)^2 |\tilde{F}_{\text{spring}}| \approx 0. \tag{7}$$

In this case, the driving force must approximately cancel the spring force, which results in a phase of 0 by which the driver leads the position. In this limit, the reasoning is the same as it is for driving an undamped oscillator at very low frequency, and the phasor diagram looks like the low-frequency limit of Fig. 5(b). These results can be coordinated with physical intuition as well: if I were to "drive" a tabletop damped mass-and-spring system at very low frequency with

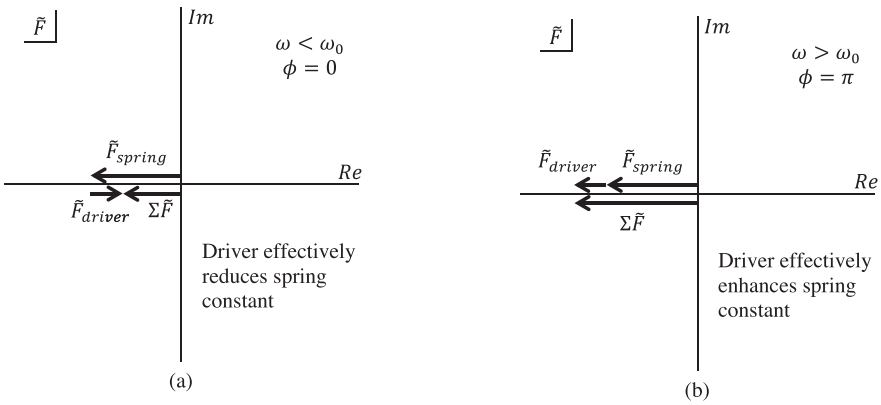

Fig. 5. Forces on an undamped oscillator with a sinusoidal driving force, shown in the complex force plane. (a) The driving frequency is less than the natural undamped frequency ω_0. (b) The driving frequency is greater than the natural undamped frequency ω_0.

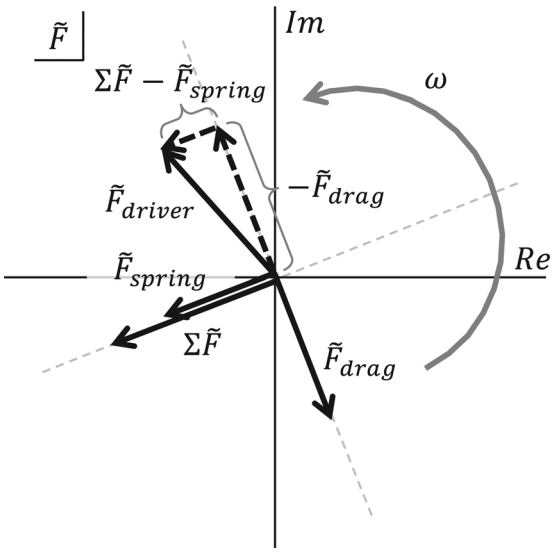

Fig. 6. Complex forces on a damped forced oscillator at some arbitrary instant during steady-state motion. The forces have constant magnitude and have constant phase angles in relation to each other, so the arrows rotate like a rigid structure at the driving frequency.

my hand, I can imagine that the effect of the driving force would be essentially to hold the mass in place at various locations, or more accurately, to move it quasi-statically with an extremely long period. In this case, it makes sense that the driving, or "holding" force, would very nearly cancel the spring force at all locations, and thus would be in phase with the position.

For the resonant frequency $\omega_r = \sqrt{\omega_0^2 - 2\gamma^2}$, the general form of the phase angle,

$$\phi(\omega) = \tan^{-1}\left(\frac{2\gamma\omega}{\omega_0^2 - \omega^2}\right), \tag{8}$$

reduces to $\phi(\omega_r) = \tan^{-1}(\omega_r/\gamma)$. If the damping is weak but non-negligible, then $\omega_r/\gamma \gg 1$ and $\tan^{-1}(\omega_r/\gamma)$ is close to, but less than, $\pi/2$, as shown in Fig. 7(b). This phase angle is consistent with the fact that the driving force must have a small positive real component to compensate for the slight excess of the spring force over the net force. The diagram indicates also that at this frequency, the driving force is approximately the same magnitude as, but slightly greater than, the damping force. In Fig. 7(c), the frequency is exactly equal to the natural frequency ω_0, the phase angle is exactly

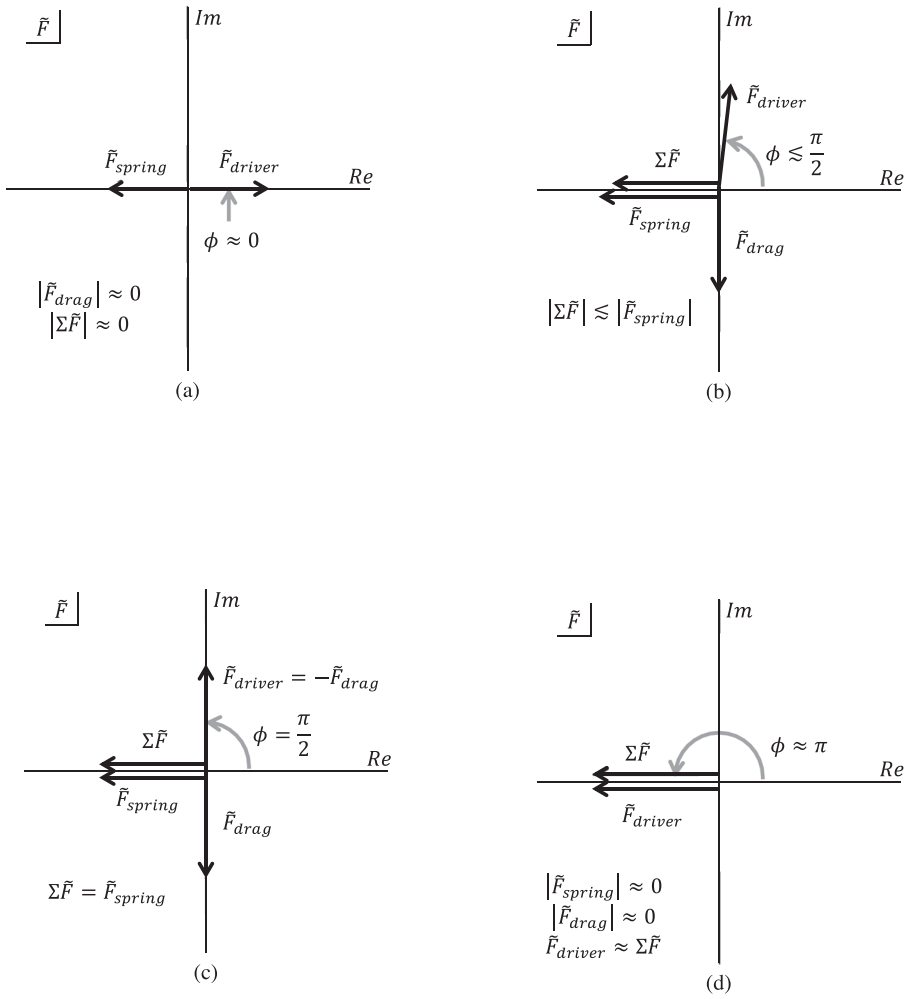

Fig. 7. Complex force diagrams for damped forced harmonic motion at different driving frequencies ω. For ease of comparison, all diagrams are shown for some instant at which the position phasor is a positive real value: (a) Very low driving frequency ($\omega \ll \omega_0$); (b) Resonance ($\omega = \omega_r = \sqrt{\omega_0^2 - 2\gamma^2}$); (c) Driving frequency equal to the natural undamped frequency ($\omega = \omega_0$); (d) Very high driving frequency ($\omega \gg \omega_0$). The scale of the diagram in (d) is "zoomed out" to keep very large forces in the frame.

$\pi/2$, and the driving force is exactly equal in magnitude to the damping force.

For very large frequency [Fig. 7(d)], the scale of the diagram is reset so that the largest forces (the driving force and the net force) are in the frame; the spring force, which does not increase with frequency, becomes relatively small. The drag force grows with frequency, but only linearly, while the net force grows quadratically. Thus, the drag force is also relatively small on this scale:

$$|\tilde{F}_{\text{spring}}| = m\omega_0^2 A_0 = m\omega_0^2 \frac{|\Sigma\tilde{F}|}{m\omega^2} \propto \left(\frac{\omega_0}{\omega}\right)^2 |\Sigma\tilde{F}| \approx 0, \quad (9)$$

$$|\tilde{F}_{\text{drag}}| = b\omega A_0 = b\omega \frac{|\Sigma\tilde{F}|}{m\omega^2} \propto \left(\frac{\gamma}{\omega}\right) |\Sigma\tilde{F}| \approx 0. \quad (10)$$

Since the net force is due mainly to the driving force, the phase angle is now almost π, which it approaches as the frequency approaches infinity. The very large frequency limit can also be checked with physical intuition in a manner similar to our imagined enactment of the very low frequency limit. In the high frequency limit, the driving force by my hand would shake the mass vigorously back and forth, with a total disregard for any haptic feedback from the natural motion of the system. This driving force would have a very large amplitude in order to achieve very high acceleration at the turning points, and because it would be very large, it would basically be achieving the acceleration by itself, without any significant help from the other available forces. Therefore, it makes sense that the phase of the driving force would be equal to that of the acceleration, and opposite to that of the position.

B. Representing $\tilde{F}_{\text{driver}}$ parametrically in the complex force plane

We can gain additional insight into the function $F(\omega)$ by plotting $\tilde{F}$ in the complex plane with the frequency ω as an independent parameter. This can be done by first following the usual steps for solving for $A(\omega)$: Substitute $\tilde{x}(t) = A_0 e^{i(\omega t-\phi)}$ into $Fe^{i\omega t} = m\ddot{\tilde{x}} + b\dot{\tilde{x}} + k\tilde{x}$, which gives $Fe^{i\phi} = m(\omega_0^2 - \omega^2)A_0 + bi\omega A_0$. The separate equations for real and imaginary parts are connected through ω, and thus they can be related

$$Re[\tilde{F}] = mA_0(\omega_0^2 - \omega^2) = mA_0\left[-\left(\frac{Im[\tilde{F}]}{2m\gamma A_0}\right)^2 + \omega_0^2\right]$$
$$= \frac{-1}{4\gamma^2 mA_0}(Im[\tilde{F}])^2 + m\omega_0^2 A_0. \quad (11)$$

We can therefore understand $Re[\tilde{F}]$ as a quadratic function of $Im[\tilde{F}]$, and we can think of $\tilde{F}$ as a parabola lying on its side, as shown in the bottom part of Fig. 8. With this perspective it is apparent from the fact that the curve is *not* perpendicular to the imaginary axis when it crosses it that the minimum magnitude of $\tilde{F}$ cannot be at $\omega = \omega_0$ but must be at some lesser frequency, where the distance from the origin to the curve is least. Figure 8 also shows the correspondence between the traditional graph $A(\omega)$, its multiplicative inverse $F(\omega)$, and the parametric graph $F(\omega)e^{i\phi(\omega)}$ in the complex plane for four frequencies, corresponding to the letters A–D. The graph can be further extended in the imagination like

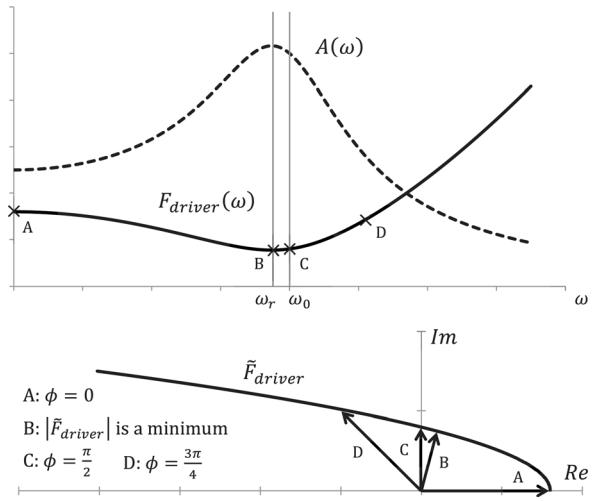

Fig. 8. Correspondence between the traditional representation of resonance $A(\omega)$ and two new alternative representations. In the top graph, $A(\omega)$ and $F_{\text{driver}}(\omega)$ are shown as real functions of the frequency ω. The graph on the bottom is the complex function $\tilde{F}_{\text{driver}}(\omega)$ shown in the complex force plane. The magnitude of this function (i.e., its distance from the origin) is the height of the graph of the real function $F_{\text{driver}}(\omega)$ in the top. In this example, $\gamma = 0.25\omega_0$.

this: Imagine a positive, real scalar field on the $\tilde{F}$ plane that is proportional to $1/F(\omega)$ and thus proportional to $A(\omega)$. If the field is represented by an "altitude" out of the plane, it would look like a circular spire that is commonly used to represent a repulsive "$1/r$" Coulomb potential. Then the graph of $A(\omega)$ in the top of Fig. 8 corresponds to the "height" above the plane along the path of the curve in the bottom of Fig. 8.

The parametric graph has several advantages: it represents a quadratic function, so it is algebraically simpler and more familiar; being parametric, it captures a higher dimensionality of information, as advised by experts in graphic design[17] (i.e., correspondence between frequency, phase, and force amplitude); and it shares a common space with the phasor diagrams of Fig. 7, which allows for opportunities for reasoning about the relationships among forces and kinematic variables. Notice that the preceding analysis still does not explain *physically* why the resonant frequency is not at the natural frequency. It may still remain as a puzzle how it can be that a slightly lower frequency should result in a greater position amplitude (or lesser force amplitude), and this despite what seems to be a slightly unfavorable phase angle that results in the driver delivering a small amount of negative power. However, by representing quantities in the complex plane, we have been able to increase the connectivity of the network of relationships among quantities and therefore have more paths of reasoning by which we can understand some of the traditional algebraic results.

VIII. CONCLUSION

In this article, I have argued that approaching harmonic motion with an emphasis on using the complex plane for geometric reasoning affords possibilities for insight and for strengthening intuition and understanding by coordinating different types of lines of reasoning, especially algebraic, physical, and geometric. By visualizing magnitudes and phase angles of complex kinematic variables and forces, how they might change over time, and how they might

change in response to a change in physical parameters such as damping constant and driving frequency, we add support to algebraic results we know and can become aware of other relationships that we did not already know algebraically. In this way, the ideas presented here can supplement and enhance the traditional practice in physics education of presenting a basic analysis of damped and forced harmonic motion to our upper-division undergraduates.

The ultimate purpose of such an approach to teaching students about harmonic motion in such fine detail is not precisely to produce students who know fine details about mathematical models for harmonic motion. Instead, the educational purpose is to provide students with a rich experience of how one can develop intimate knowledge of a physical system or model through the discipline of coordinating multiple representations and lines of reasoning. Through this experience, it may be that students will be better prepared to forge such relationships for themselves and their peers with newly discovered physical systems and models.

ACKNOWLEDGMENTS

The author thanks Bradley Ambrose and Michael Wittmann, first, for their development of *Intermediate Mechanics Tutorials,* which inspired the work the author reports here, and second, for their careful readings of the manuscript. Eleanor Close also made helpful suggestions for clarifying the manuscript.

[1]See, for example, S. Goldin-Meadow and S. Beilock, "Action's influence on thought: The case of gesture," Perspect. Psychol. Sci. **5**(6), 664–674 (2010); R. E. Scherr, H. G. Close, E. W. Close, V. J. Flood, S. B. McKagan, A. D. Robertson, L. Seeley, M. C. Wittmann, and S. Vokos, "Negotiating energy dynamics through embodied action in a materially structured environment," Phys. Rev. Spec. Top. Phys. Educ. Res. **9**, 020105-1–18 (2013); R. Lindgren and M. Johnson-Glenberg, "Emboldened by embodiment: Six precepts for research on embodied learning and mixed reality," Educ. Res. **42**(8), 445–452 (2013).

[2]P. B. Kohl, D. Rosengrant, and N. D. Finkelstein, "Strongly and weakly directed approaches to teaching multiple representation use in physics," Phys. Rev. Spec. Top. Phys. Educ. Res. **3**, 010108-1–10 (2007).

[3]A. Van Heuvelen and X. Zou, "Multiple representations of work-energy processes," Am. J. Phys. **69**(2), 184–194 (2001).

[4]R. B. Kozma, "The material features of multiple representations and their cognitive and social affordances for science understanding," Learn. Instrum. **13**(2), 205–226 (2003).

[5]P. B. Kohl and N. D. Finkelstein, "Patterns of multiple representation use by experts and novices during physics problem solving," Phys. Rev. Spec. Top. Phys. Educ. Res. **4**, 010111-1–13 (2008).

[6]B. S. Ambrose, "Investigating student understanding in intermediate mechanics: Identifying the need for a tutorial approach to instruction," Am. J. Phys. **72**(4), 453–459 (2003).

[7]R. E. Pepper, S. V. Chasteen, S. J. Pollock, and K. K. Perkins, "Observations on student difficulties with mathematics in upper-division electricity and magnetism," Phys. Rev. Spec. Top. Phys. Educ. Res. **8**, 010111 (2012).

[8]C. A. Manogue and E. Gire, "Cognitive development at the middle-division level," AIP Conf. Proc. **1179**, 19 (2009); C. A. Manogue, P. J. Siemens, J. Tate, K. Browne, M. L. Niess, and A. J. Wolfer, "Paradigms in Physics: A new upper-division curriculum," Am. J. Phys. **69**(9), 978–990 (2001).

[9]C. Singh, "Interactive learning tutorials on quantum mechanics," Am. J. Phys. **76**(4), 400–405 (2008).

[10]S. V. Chasteen, S. J. Pollock, R. E. Pepper, and K. K. Perkins, "Transforming the junior level: Outcomes from instruction and research in E&M," Phys. Rev. Spec. Top. Phys. Educ. Res. **8**, 020107-1–18 (2012).

[11]J. B. Marion and S. T. Thornton, *Classical Dynamics of Particles and Systems*, 3rd ed. (Harcourt Brace Jovanovich, San Diego, 1988).

[12]J. R. Taylor, *Classical Mechanics* (University Science Books, Herndon, VA, 2005).

[13]Taylor, Ref. 12, p. 184.

[14]D. Halliday, R. Resnick, and J. Walker, *Fundamentals of Physics*, 9th ed. (Wiley, Hoboken, NJ, 2011); R. Knight, *Physics for Scientists and Engineers: A Strategic Approach with Modern Physics*, 3rd ed. (Pearson, New York, 2012).

[15]A. Sfard, "On the dual nature of mathematical conceptions: Reflections on processes and objects as different sides of the same coin," Educ. Stud. Math. **22**(1), 1–36 (1991).

[16]D. L. Schwartz and J. B. Black, "Shuttling between depictive models and abstract rules: Induction and fallback," Cogn. Sci. **20**, 457–497 (1996).

[17]E. Tufte, *Beautiful Evidence* (Graphics Press, Cheshire, CT, 2006), p. 129.